Journal of Petroleum Science and Engineering 172 (2019) 1202–1214

Contents lists available at ScienceDirect

Journal of Petroleum Science and Engineering

journal homepage: www.elsevier.com/locate/petrol

Experimental study on water sensitivity and salt sensitivity of lignite reservoir under different pH

Boyang Wang[a,b], Yong Qin[a,*], Jian Shen[a], Gang Wang[c], Qiusheng Zhang[d], Miao Liu[e]

[a] Key Laboratory of Coalbed Methane Resources and Reservoir Formation Process of the Ministry of Education, China University of Mining and Technology, Xuzhou, 221116, China

[b] Accumulation and Development of Unconventional Oil and Gas, State Key Laboratory Cultivation Base Jointly-constructed by Heilongjiang Province, Ministry of Science and Technology, Northeast Petroleum University, Daqing, 163318, China

[c] School of Earth Science and Engineering, Hebei University of Engineering, 056038, China

[d] Suzhou NanZee Sensing Technology Co.,Ltd, Suzhou, 215123, China

[e] Daqing Oil Field Co, Daqing, 163000, China

ARTICLE INFO

Keywords:
Lignite reservoirs
Water sensitivity
Salt sensitivity
pH

ABSTRACT

The water sensitivity and salt sensitivity of lignite reservoirs are important factors affecting the productivity of the coalbed methane (CBM) well. This paper took the lignite of Erlian Basin as the research object. The content and occurrence of mineral was analyzed by LTA + XRD combined with scanning electron microscopy (SEM), and distribution of each functional group of lignite was analyzed by infra-red spectrum. Based on the above analysis, standard salt water with different pH and salinity was used as the experimental injection fluid, and water sensitivity (salt sensitivity) experiments were performed under the condition of constant effective stress. The experimental results show that the sample contains a large number of water-sensitive minerals (kaolinite and illite/smectite mixed layer mineral), and the ratio of carbonyl, hydroxybenzene and carboxyl groups is 10:7:1. Hydrogen bonds are mainly OH···N hydrogen bonds. The lignite reservoirs with different pH have different degrees of water-sensitive damage, and the damage rates from high to low are partial alkalinity conditions (54.18%), partial acidity conditions (42.6%), and strong alkalinity conditions (23.67%). The dimensionless permeability changes with the decrease of salinity, which can be divided into three stages (no water sensitivity stage, particle migration water sensitivity stage, particle expansion water sensitivity stage) with 1250 mg/L and 10000 mg/L as the boundary. The displacement pressure and pH are the main controlling factors at different stages, and pH controls the wettability of pulverized coal and the hydration expansibility of clay minerals. The dimensionless permeability of lignite reservoir increases with the increase of salinity under the acidic condition. Under alkaline conditions, it is characterized by no-weak salt sensitivity. The greater the alkalinity, the stronger the salt sensitivity, which is mainly controlled by the change of the thickness of the water film under the influence of pH.

1. Introduction

In the process of CBM development, coal reservoirs will contact drilling fluid, fracturing fluid and other external fluids. If these external fluids do not match the fluids or mineral properties of the reservoir, physical and chemical reactions can occur, possibly leading to a decrease of reservoir seepage capacity and affecting the productivity of the CBM well to varying degrees (Moghanloo et al., 2015). Coal reservoirs are sensitive to a number of variables, including velocity, stress, water, salt, acid, alkali and others (Ma et al., 2016). Some scholars (Geng et al., 2017a,b; Tao et al., 2017) have performed research on velocity sensitivity and stress sensitivity and have basically reached a consensus. It is believed that the dispersion and movement of coal particles and the generally strong stress sensitivity of coal reservoirs are the main factors that lead to a serious reduction of the permeability of coalbed methane reservoirs during the drainage process. However, there are few reports on the other sensitivities of coal reservoirs, which is one of the major reasons that the commercial development of coalbed methane in China is restricted. For low rank coal in China with low permeability (generally 2 to 4 orders of magnitude lower than common CBM reservoirs), hydraulic fracturing operations are required in the early stage to increase the production rate of coalbed

* Corresponding author.
E-mail address: yongqin@cumt.edu.cn (Y. Qin).

https://doi.org/10.1016/j.petrol.2018.09.036
Received 16 March 2018; Received in revised form 30 August 2018; Accepted 10 September 2018
Available online 11 September 2018
0920-4105/

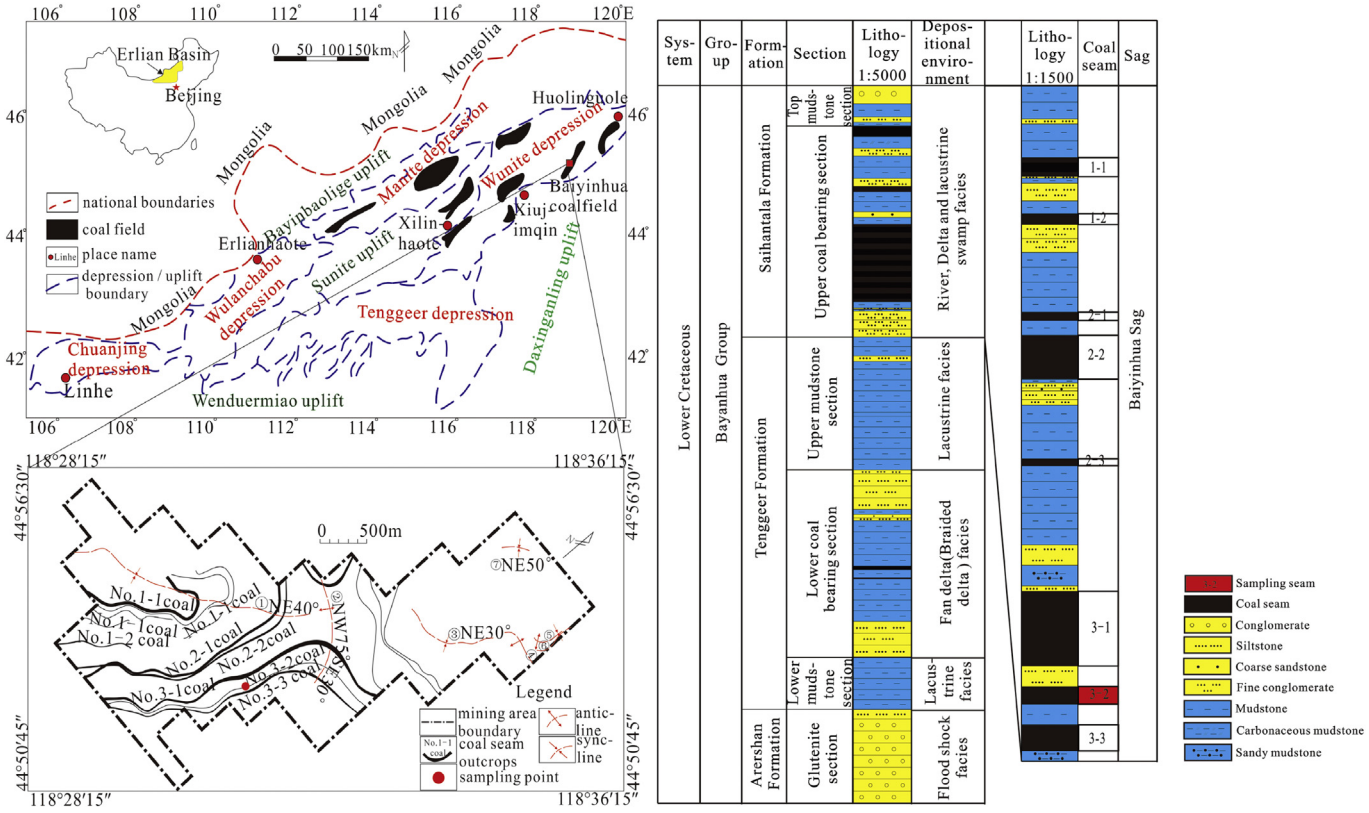

Fig. 1. Sampling locations and coal stratigraphy.

methane (Huang et al., 2017). However, the injection of fracturing fluid can damage the coal reservoir, for example, the clay components in coal react with the filtrate of the fracturing fluid and expand, resulting in a decrease of permeability. This decrease in permeability is extremely difficult to reverse (Tan et al., 1997). Most coalbed methane wells in China are made by drilling with clear water and fracturing with a freshwater-based fracturing fluid, which results in a significant lack of attention to reservoir damage. Reservoir sensitivities, such as water sensitivity, are more detrimental to low permeability coal reservoirs (Zou et al., 2014).

Currently, the study of water sensitivity shows the expansion of clay minerals under low salinity conditions (particle expansion water sensitivity) and the blocking of pores by particle migration under the action of fluids (particle migration water sensitivity), which are the primary causes of water sensitivity (Khilar and Fogler, 1984). The factors that affect the water sensitive effect can be divided into internal factors (reservoir pore structure characteristics, mineral composition and content, occurrence forms) and external factors, which lead to changes of the reservoir pore structure or the original state of the fluid (pH, displacement pressure difference) (Wang et al., 2001; Wei, 2014). In previous studies, attention was mainly paid to the influence of internal factors on water sensitivity effects (Geng et al., 2017a,b). Few scholars have conducted studies on the response of external factors to the water sensitive effect, especially experimental studies under the coupling condition of double factors. Bai (2014) proposed that during the process of CBM well drainage, there is little change in the anions, cations and pH values of coal seam water. Therefore, the most prominent impact on drainage is the sensitivities of the flow velocity and stress. However, external fluids with different pH values affect not only the minerals that are responding to them but also the agglomeration and migration of pulverized coal particles, which affect the strength of the water sensitivity effect (Shi et al., 2018).

Due to the hydration of non-expanding minerals such as kaolinite, it is very easy to form loose granular debris from the shear force of high speed fluid, which are transported with the fluid to block pores and lead to the migration of water sensitivity. Therefore, the height of the displacement pressure is one of the key factors that affect the strength of the water sensitive effect. Some scholars (Wang et al., 2001; Geng et al., 2017a,b) attempted to explore the influence of differing liquid flow rates and pH values on the water sensitivity of rocks, but the research objects were mostly high rank coal and sandstone reservoirs. A sensitivity study of low rank coal, such as a lignite reservoir, has not yet been performed. Previous studies have focused on the influence of inorganic components (clay minerals) on reservoir sensitivity, while ignoring the influence of the organic composition (pulverized coal) (Wang et al., 2001; Geng et al., 2017a,b). Due to the extremely low permeability of coal reservoirs, some scholars have tried to use nitrogen instead of water as a fluid medium to measure the permeability of coal rock, which is not only inconsistent with the actual reservoir conditions but also ignores the impact of the water-rock interaction (Zuo et al., 2014).

Due to the above reasons, samples of lignite from the Erlian basin were collected for this study. Standard brine with various pH values and salinities is used as the experimental injecting liquid, and water sensitivity and salt sensitivity experiments are carried out under constant effective stress conditions. The influence of different displacement pressure and pH conditions on sensitivity is analyzed from two facets: the compositions of organic and inorganic minerals, with the aim of determining the mechanisms of water sensitivity and salt sensitivity of lignite reservoirs under comprehensive influence factors and providing a theoretical basis for strengthening the protection of low rank coal reservoirs.

2. Experimental

2.1. Geological background

The Erlian Basin is a Mesozoic rift basin on the Inner Mongolia–Daxinganling Hercynian fold basemen. It is located in

central-northern Inner Mongolia, China and is surrounded by the Daxinganling to the east, the Wulatehouqi to the west, the Yin Mountains to the south, and the China–Mongolia border to the north. The Erlian Basin is one of the largest onshore sedimentary basins in China and comprises five depressions and an uplift. The Baiyinhua coalfield is located in the northeast of the Erlian Basin, and it covers an area of 600 km^2. The opencast coal mine is in the middle of the coalfield, and its main structural feature is an incomplete wide and gentle syncline (Wang et al., 2018). In addition, the coalfield is characterized by seven secondary folds, although no faults are found within it (Fig. 1). The main coal-bearing strata are the Shengli Formation and Xilin Formation of the Early Cretaceous Bayanhuaqun group. At present, only the upper coal-bearing section of the Bayanhuaqun group has been exploited; those are (from top to bottom) the No.1 coal group, No.2 coal group, and No.3 coal group, which are divided into eight coal seams (Fig. 1). Of those, the No.3 coal group is the most stable recoverable coal seam in the entire area and has a thickness ranging from 0.85 to 39.84 m with an average of 18.31 m.

2.2. Sample collection and processing

The sampling point in this study is located in the middle of the Baiyinhua coalfield, and No.3–2 coal under exploitation was selected as the research object, the thickness of which is between 0.15 m and 17.75 m (average 1.13 m). A cylindrical coal sample of 25 mm (diameter) × 50 mm (length) was drilled for a speed sensitive evaluation test at a core direction parallel to the bedding direction; the coal samples drilled were all original structural coal. According to the national standard, the sample at the end of the coal pillar should be used to conduct an industrial analysis, elemental analysis, total sulfur and sulfur analysis, maceral quantification, and R_o test. Low-temperature ash (LTA) was obtained by ashing the coal samples using an EMITECH K1050X plasma asher at < 200 °C until the mass difference was less than 1%. Ash samples were milled and passed through a 200-mesh sieve. X-ray diffraction analysis of LTA was performed using a Bruker D8-Discover X-ray diffractometer at 40 kV and 40 mA, with a scanning angle of 3°–45°. The relative clay content was determined using the suspension method. Clay minerals with a diameter of less than 2 μm were extracted, and a directional film was produced that included natural air dried pieces, ethylene glycol pieces, and pieces heated at 550 °C. The diffraction peak intensity contrast method and adiabatic equations were subsequently used to calculate the clay mineral content (Jozanikohan et al., 2016). The instrument used in the FTIR test is Nicolet 6700 Fourier transform infrared spectrometer (the resolution is 4 cm^{-1}, the number of scanning times is 32 times, and the spectrum range is 4000–400 cm^{-1}), which is processed by KBr compression method. The minerals of lignite was observed with FEI Quanta 450FEG high resolution field emission scanning electron microscopy (SEM) under the low vacuum non conducting mode. According to basic test results, samples with a similar material composition were selected to conduct sensitivity experiments.

2.3. Experimental methods

According to 48 salinity and 18 pH data points collected from four major low-rank coal basins (Tuha Basin, Junggar Basin, Hailar Basin, and Erlian Basin) (Huang et al., 2005; Wang, 2010; Deng, 2015), the pH values were mainly distributed between 7 and 9, with an average of 8. Therefore, the three levels of pH were set as 6, 8, and 10 (Fig. 2, Table 1). The salinity data were divided into three categories: below 1000 mg/L, 1000 mg/L to 4000 mg/L, and greater than 4000 mg/L (each range represents approximately 1/3 of the sample population) (Table 1). The mean value of salinity less than 1000 mg/L was 453.8 mg/L, representing the minimum value. The mean value of salinity less than 4000 mg/L was 1243.8 mg/L, representing the overall average and accounting for 68.75% of all of the salinity data. The mean value of salinity greater than 4000 mg/L was 14,391.7 mg/L, representing the maximum value. The maximum value of water sensitive mineralization and the minimum salinity of salt sensitivity were set to 14400 mg/L (Table 1). The degree of salinity in the water sensitive experiments was set in the order of 14400 mg/L, 10000 mg/L, 5000 mg/L, 1250 mg/L, 450 mg/L and distilled water. The salinity sensitivity in salt sensitive experiments was set in the order of 60000 mg/L, 40000 mg/L, 20000 mg/L and 14400 mg/L. The injection fluid was of standard salinity ($NaCl:CaCl_2:MgCl_2{\cdot}6H_2O$ = 7:0.6:0.4) with various mineralization degrees and pH values. The injection fluid was configured as follows. First, a water solution with different salinities was configured, the pH of which was measured using a PHS-3C acidity meter. HCl (0.5 mol/L) and NaOH (0.5 mol/L) were used to regulate the pH of the solution. After each configuration, hydrochloric acid or sodium hydroxide was added. The solution was stirred evenly with a glass rod and then measured with a PHS-3C acidity meter. This process was repeated until the pH (6, 8, 10) set described in the text was reached. After each pH measurement, the glass electrodes was cleaned to ensure the accuracy of the pH determination. The configured liquid was filtered by suction and then placed in an intermediate container (200 ml) for displacement using an ISCO pump (Fig. 3). The displacement process was carried out by controlling the displacement pressure, and the displacement volume depended on physical parameters, such as coal reservoir porosity.

Before carrying out the coal reservoir water sensitivity (salt sensitivity) experiment, velocity sensitivity evaluation experiment was conducted to estimate a reasonable flow rate condition. The water sensitivity and salt sensitivity experiments were carried out under constant effective stress conditions. The present buried depth of the brown coal seams in these basins is less than 1200 m (Wang, 2010; Deng, 2015), and considering the influence of the gas weathering zone, the effective stress was set to 8 MPa. The experimental conditions are shown in Table 2.

Zeta test methods: Pulverized coal (clay minerals) was added to experimental fluid with a configured salinity of 200 mL (solid/liquid mass percentage, 1%). The ultrasonic wave oscillated at 30 s to fully disperse the solid phase. The pH value of the solution was adjusted unidirectionally with 0.5 mol/L HCl and 0.5 mol/L NaOH after the liquid was loaded into the measuring container. That is, pH value of the solution was adjusted from the initial pH value to approximately 2(6), and then, the same unmeasured was is used to adjust the pH value to 12. The measurements of the zeta potential were repeated three times at each set pH point, and the average was taken as the final result (Yu et al., 2011; Li et al., 2014). The experimental instrument was a Zeta Probe potentiometer produced by Colloidal Dynamics, USA.

2.4. Water sensitivity (salt sensitivity) evaluation method

Fluid pressure (P_f) is calculated as follows (Li et al., 2013):

$$P_f = \frac{P_{in} + P_{out}}{2} \tag{1}$$

The effective stress is calculated as follows (Wu et al., 2017):

$$P_e = \sigma - P_f \tag{2}$$

Note: P_e – effective stress, σ – confining pressure, MPa; P_f – pore fluid pressure, MPa; P_{in} – inlet pressure, MPa; P_{out} – outlet pressure, MPa.

The experiment used the steady-state method for testing. Thus, fluid permeability can be obtained by Darcy's law.

$$Q = KA\frac{\Delta P}{\mu L} \tag{3}$$

Note: K – fluid permeability, μm^2 (D); Q – flow, cm^3/s; μ – fluid viscosity, MPa·s; L – core length, cm; A – cross-sectional area of coal sample, cm^2; ΔP – differential pressure on both ends of the coal sample, 10^5 Pa.

The water sensitive damage rate (D_w) is expressed as:

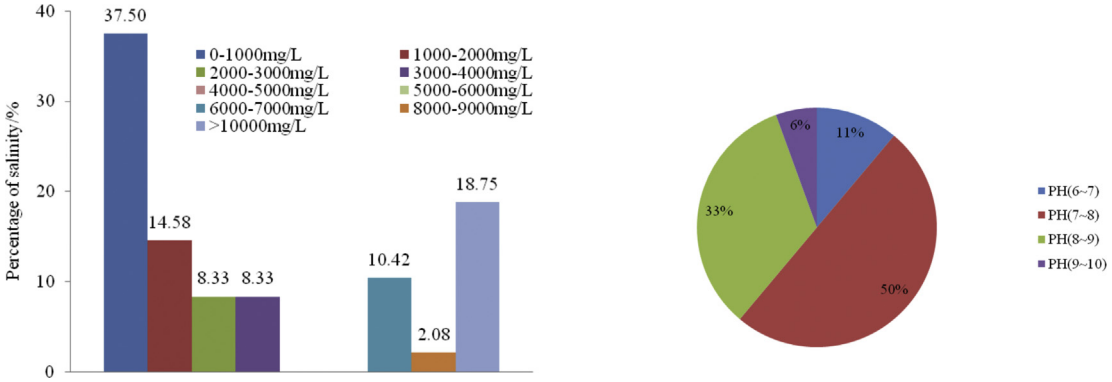

Fig. 2. Salinity and pH statistical results of the formation water in low-rank coal basins of China.

$$D_w = \frac{|K_i - K_w|}{K_i} \quad (4)$$

Note: K_w – permeability under distilled water conditions, K_i – permeability under formation water conditions.

The salt sensitive damage rate (D_w) is expressed as:

$$D_v = \frac{|K_i - K_s|}{K_i} \quad (5)$$

Note: K_s – permeability under the highest salinity conditions, K_i – permeability under formation water conditions.

According to the Chinese oil industry standard SY/T 5358-2010, the water (salt) sensitive damage rate is less than 5%, 5%–40%, 40%–70%, 70%–90% corresponding to no water (salt) sensitivity, weak water (salt) sensitivity, medium-strong water (salt) sensitivity, strong water (salt) sensitivity, respectively.

3. Results and discussion

3.1. Material composition of coal

The results reveal that the coal samples are low-ash coal with a high moisture content (Table 3). The content of huminite is the highest (75.4%) and is dominated by ulminite. There is also lower content of inertinite (5.2%) and liptinite (18.98%). The minerals are mainly clay and quartz (Table 3). The XRD results of LTA showed that the minerals in coal are dominated by clay followed by quartz. The clay minerals are dominated by kaolinite and illite/smectite mixed layer (Table 4, Fig. 4).

Kaolinite is associated with organic matter and occurs as curved worm-like and laminated structures (Fig. 5a and b), while illite is filled in the pores in a plate form (Fig. 5c and d). The I/S mixed layer mineral is attached to the surface of the coal matrix in a net shape (Fig. 5e), and quartz is mostly distributed in huminite in a dispersive manner (Fig. 5f). Various types of clay minerals have various effects on water sensitivity. Among them, illite occurs as lamellar or in strips filling in fractures After expanding, illite can block the percolation channel, reducing reservoir permeability. I/S is a mixed layer mineral that attaches to the surface of the coal matrix in a net shape, which can be loosely disintegrated and even broken after hydration, causing particle migration, which decreases permeability. Kaolinite can cause the loss and migration of clay mineral particles under the action of fluid shear, resulting in permeability damage (Geng et al., 2017a,b).

3.2. Analysis of the structural characteristics of lignite

The ability to analyse the chemical structure of coal by FTIR and the peak separation technique has been recognized by most scholars (Chen et al., 2012; Zhang et al., 2016). In the actual infrared spectrum, as the absorption bands of many functional groups in coal contribute to the infrared spectrum, it is very easy to produce overlapping peaks at a certain location, making it difficult to determine the absorption peaks and their boundaries. In this paper, the obtained infrared spectrum curve is fitted by Gaussian partial peaks(Chen et al., 2012; Zhang et al., 2016; He et al., 2017; Zhu et al., 2018). According to the theory of infrared spectroscopy and organic chemistry, four types of absorption peaks (hydroxyl, aliphatic hydrocarbon, oxygen-containing functional groups, aromatic structure) are quantified, which correspond to wave numbers as shown in Fig. 8a.

The hydroxyl in coal is an important functional group that affects the reactivity of coal. The absorption peak is mainly between 3650 cm^{-1} and 3000 cm^{-1}. According to the hydrogen bond classification of hydroxyl groups in coal proposed by Painter et al. (1987), the number of wave numbers from large to small is free OH hydrogen bonds, OH-π hydrogen bonds formed by the π electron on the aromatic nucleus, hydrogen bonds formed by the hydroxyl group of self associating hydroxyls, OH-ether hydrogen bonds formed by the action of ether, hydrogen bonds of the ring structure, and OH-N hydrogen bonds. Because of the low degree of coalification of lignite and greater number of oxygen functional groups in coal, the effect of various hydrogen bonds is stronger. The results show that six types of hydroxyl groups and their hydrogen bonds exist at the same time (Fig. 8b). The content of the OH-N hydrogen bond is far greater than that of the other hydrogen bond types, followed by the hydrogen bonds of the ring structures (Table 6).

Lignite from different depressions in the Erlian Basin (Baiyinhua depression, Huolinhe depression, Shengli depression) were selected for FTIR and ultimate analysis (Table 5). H-14 as collected from the No.14 coal seam in the Huolinhe south open-pit mine, S-5a and S-5b were collected from the No.5 and No.5_{lower} coal seam of the Xi-2 minefield of the Shengli coalfield, and B-3b was collected from the No.3-2 coal seam of the Baiyinhua No. 3 open pit mine. The collected samples were crushed to a diameter of less than 0.25 mm, weighed (approximately 100 g), placed in an incubator containing a supersaturated K_2SO_4 solution, and wetted until a constant weight was achieved. The balanced

Table 1
Salinity and pH statistical results of the formation water in low-rank coal basins of China.

Salinity range (mol/L)	Number	Mean value (mol/L)	Ratio (%)	pH range	Number	Mean value	Ratio (%)
0–0.017	18	0.008	37.5	6–7	2	6.67	11
0.017–0.068	15	0.021	31.25	7–9	15	7.96	83.3
0.068–0.62	15	0.246	31.25	9–10	1	9.6	5.7

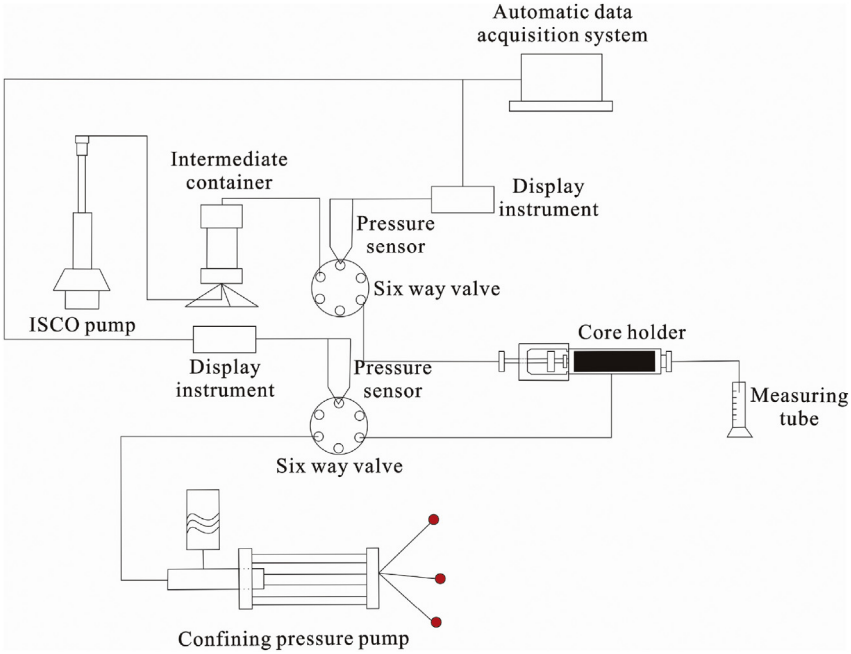

Fig. 3. Reservoir sensitivity analyzer.

Table 2
Constant effective stress experimental conditions at different pH.

Number	Injection pressure/ MPa	Confining pressure/ MPa	Effective stress/ MPa	pH
1	5.6	10.8	8	6
2	8.8	12.4	8	8
3	6.2	11.1	8	10

Table 3
Basic information of the BYH-3-2 coal sample.

Ultimate analysis	O_{daf} (%)	C_{daf} (%)	H_{daf} (%)	N_{daf} (%)	$S_{t,d}$ (%)
	25.27	70.99	1.1	1.55	0.95
XRD	Kaolinite (%)	Illite(%)	I/S(%)	Quartz(%)	Calcite(%)
	36.57	4.14	24.29	30	5
Proximate analysis and $R_{o,max}$ test	M_{ad} (%)	A_{ad} (%)	V_{ad} (%)	FC_{ad} (%)	R_o (%)
	32.44	8.68	28.55	30.33	0.35

Note: I/S - illite/smectite mixed layer mineral, *ad* - air dried basis, *daf* - dry ash free basis, *d* - dry basis.

Table 4
Results of the coal quality analysis performed on the BYH-3-2 coal sample.

Maceral with mineral matter/%					
Huminite	Textinite	9.36	Liptinite	Sporinite	7.28
	Ulminite	30.68		Cutinite	5.2
	Attrinite	7.28		Resinite	2.34
	Desinite	1.04		Suberinite	2.86
	Gelinite	12.48		Alginite	0
	Corpohuminite	14.56		Liptodetrinite	1.3
Inertinite	Fusinite	3.12		Chlorophyllinite	0
	Semifusinite	0.26		Biturninite	0
	Macrinite	0.78	Mineral matter	Clay mineral	0.31
	Micrinite	0		Sulfide	0
	Sclerolinite	0		Carbonate	0.11
	Inertodetrinite	1.04		Oxide	0.00

water content was then measured. The balanced water content from high to low was B-3b, S-5a, S-5b, and H-14. Fig. 6 shows the peak fitting results of the hydroxyl groups of four experimental coal samples. From the results of the partial peak fitting and ultimate analysis, the content of the OH-N hydrogen bond is mainly positively correlated with the nitrogen content (Figs. 6 and 7). Previous studies have shown that for coal in the same era, the trend of the nitrogen content change in coal is reduced with increasing coalification (Chen, 1988). Since the coals selected in this paper are all lignite, the coal level has a weak control of the nitrogen content. The reduction degree of peat swamp has an important effect on the nitrogen content in coal (Chen, 1988). The weaker the reduction degree of the coal, the lower the nitrogen content of the coal is due to the oxidation of nitrogen and the decomposition of NO_x gas. The content of the OH-N hydrogen bond is mainly positively correlated with the water content (Fig. 7). The greater the water content, the stronger the water sensitivity. Because of the low content of the carboxyl group, the main factor affecting the wettability of the coal surface is the hydroxyl group (Pietrzak and Wachowska, 2006), and the hydroxyl nitrogen hydrogen bond is the main controlling factor, because other types of hydroxyl hydrogen bonds have no obvious correlation to water.

The content of aliphatic hydrocarbons in coal is mainly reflected in the range of wave numbers from 3000 cm^{-1} to 2700 cm^{-1}. There are symmetric and asymmetric telescopic vibrations of saturated hydrocarbon CH_2 (2855 cm^{-1}, 2925 cm^{-1}), symmetric and asymmetric telescopic vibration of CH_3 (2871 cm^{-1}, 2955 cm^{-1}), and a telescopic vibration of CH (2890 cm^{-1}) (Machnikowska et al., 2002). The results show that the asymmetry extension vibration peak of CH_x is greater than a symmetrical extension vibration peak. The methylene content is higher, followed by the concentration of methyl groups, indicating that fatty hydrocarbons are mainly in the form of long chains (Fig. 8c, Table 7).

The oxygen functional groups in coal include the hydroxyl group, carboxyl group, carbonyl group and ether oxygen. The peak of the latter three are mainly between 1800 cm^{-1} and 1000 cm^{-1}. There is a weak acromion near 1700 cm^{-1}, indicating that there are carboxylic acid groups in lignite, but the content is relatively low. The absorption peak near 1600 cm^{-1} is strong, which indicates that the contents of phenol and ether are higher in coal samples. The ratio of the relative vibration area of the above two is 20.32: 3.09, indicating that the ratio of carbonyl group and the carboxyl ratio is approximately 7 (Robertson, 2004). The C-O vibration of hydroxyl benzene and ether were indicated at 1109.93 cm^{-1}, 1136.08 cm^{-1} and 1197.74 cm^{-1}. The ratio of the

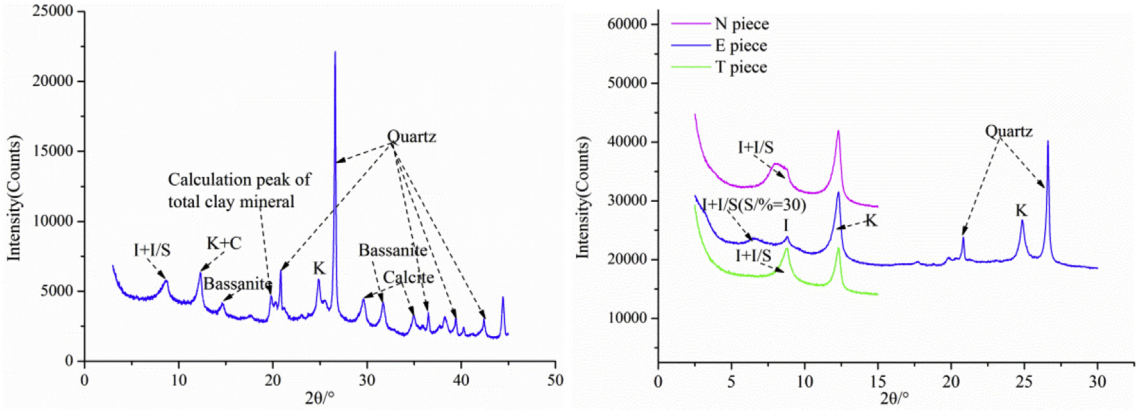

Fig. 4. Whole-rock and clay minerals XRD spectra of BYH-3-2 LTA.

vibrational area among hydroxyl benzene, ether C-O and unsaturated carboxylic acids is 10. Therefore, the ratio of the carbonyl, hydroxyl benzene and carboxyl is 10:7:1 (Fig. 8d, Table 8).

The low wave number region between 700 cm^{-1} and 900 cm^{-1} is the vibrational peak of the aromatic structure in the infrared spectrum of coal. The results show that there are four substitutions in the benzene ring, which is dominated by four substitutions of the benzene ring (2H) and five substitutions of the benzene ring (1H) (Fig. 8e, Table 9).

3.3. Water sensitive damage and its mechanism

The results of the water sensitivity experiments show that the lignite reservoirs under various pH values display different degrees of water sensitivity damage. The damage rate, from high to low, is partial alkalinity (54.18%), partial acidity (42.6%) and strong alkalinity condition (23.67%). According to section 2.4, the former two are strong water sensitive and the latter is weak water sensitive (Fig. 9a). The change of the non-dimensional permeability rate with the decrease of salinity shows three stages with two key points, M_1 and M_2, as boundaries. In the first stage, the non-dimensional permeability showed a downward trend under acidic conditions, and almost no change under alkaline conditions. The higher the alkalinity, the more unchanged the permeability., indicating that pH is the main controlling factor at this stage. Previous studies have suggested that adding acid will reduce the hydrophilicity of the lignite surface, and because the wetting heat of minerals is much lower than the heat of organic matter in coal, the acid solution will dissolve some small molecules (Pietrzak and Wachowska, 2006; Liu et al., 2017). Therefore, the dissolution of some small molecules containing oxygen-containing functional groups by the acid solution is an important cause of the decrease in hydrophilicity. Combined with the infrared spectroscopy results, it is observed that, due to the low degree of coalification of lignite, there are a large number of oxygen-containing groups on the surface, such as hydroxyl, carboxyl, carbonyl and ether oxygen. Among these factors, the carboxyl content is the most important factor that affects the surface wettability of coal, followed by hydroxyl. It is observed from the chemical structure that

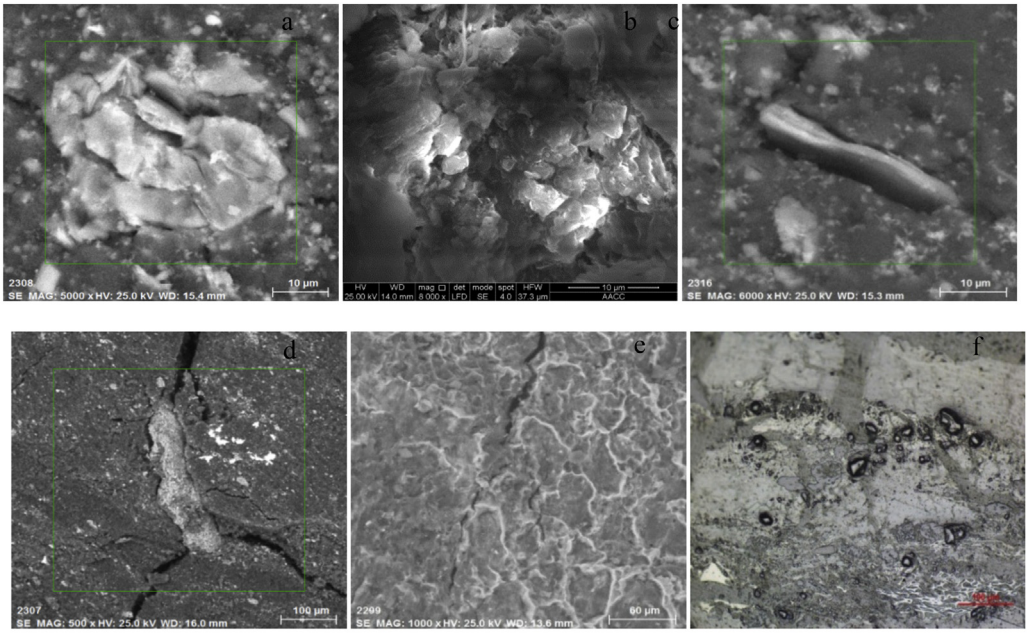

(a) Kaolinite with curved worm-like (b) Kaolinite with laminated (c) Illite filled in the pores (d) Illite in plate form (e) I/S mixed layer mineral attached to the surface of the coal matrix(f) Quartz in a dispersive form

Fig. 5. Characteristics of mineral occurrence under scanning electron microscope and optical microscope.

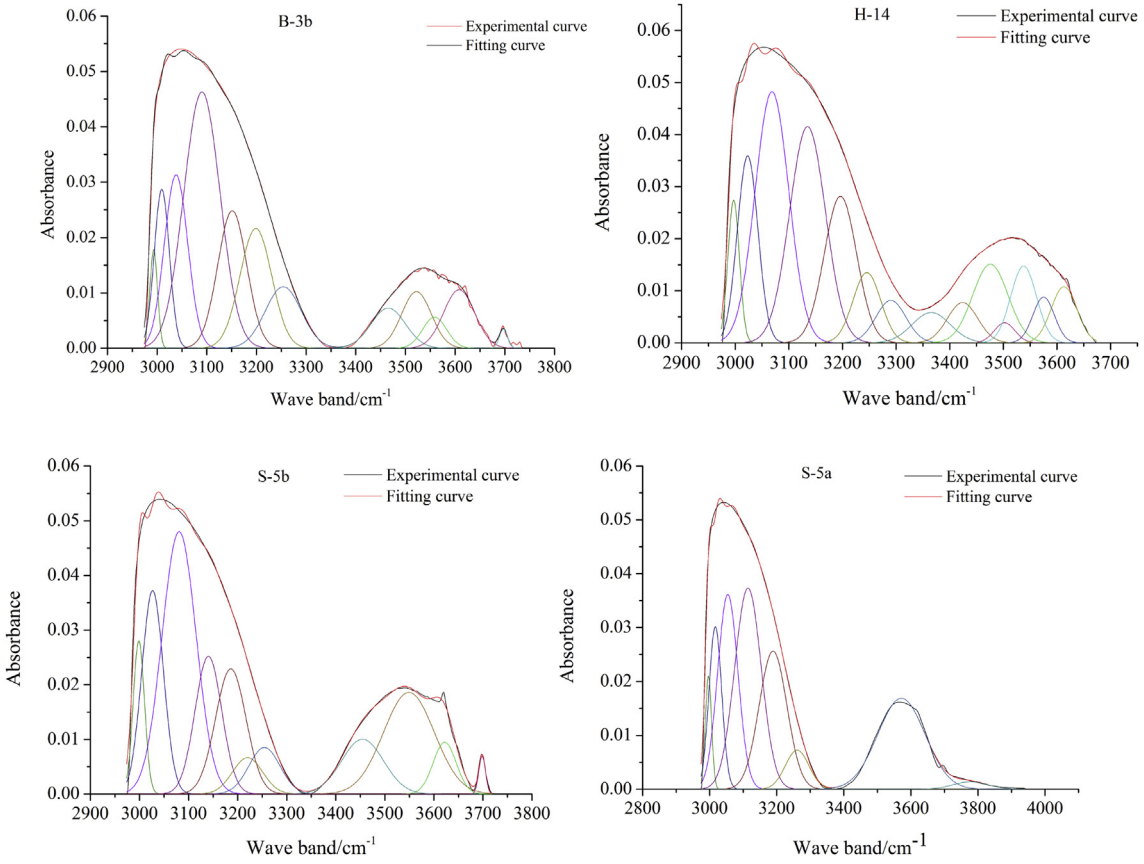

Fig. 6. Peak fitting diagram of hydroxyl absorption band.

carbonyl and ether groups have little influence on wettability and have no correlation with the contact angle (Cuntian, 1992). Compared to high-rank coals, the carboxyl and hydroxyl contents of lignite are significantly higher, which is more sensitive to the above-mentioned phenomena. In conclusion, compared to the alkaline condition, the concentration of pulverized coal in the acidic condition leads to a significant decrease in permeability in the first stage.

As the salinity is further reduced, the dimensionless permeability begins to decline under alkaline conditions, indicating that the water sensitive damage begins and enters the second stage (Fig. 9a). Research shows that water sensitivity effect is mainly affected by the influence of clay minerals. Kaolinite and illite can lead to particle migration water sensitivity, and an illite/smectite mixed layer and montmorillonite can lead to expansion of particle water sensitivity (Zhu et al., 2004; Liao et al., 2012). The XRD results of LTA showed that the clay minerals are dominated by kaolinite and illite/smectite mixed layer, so water sensitive damage should include these parts. In the second stage, the damage rate of dimensionless permeability from high to low is partial alkalinity, strong alkalinity and partial alkalinity, which has a good positive correlation with the displacement pressure (Fig. 9b). It is indicated that kaolinite and illite are more likely to disperse into loose granular debris under the shear force of the fluid, which is transported with the fluid to clog the pores. This stage is mainly determined by the strength of the particle migration water sensitivity. From the perspective of mechanics, Van Der Waals force between kaolinite and the coal matrix is larger than the double layer repulsion force under the water

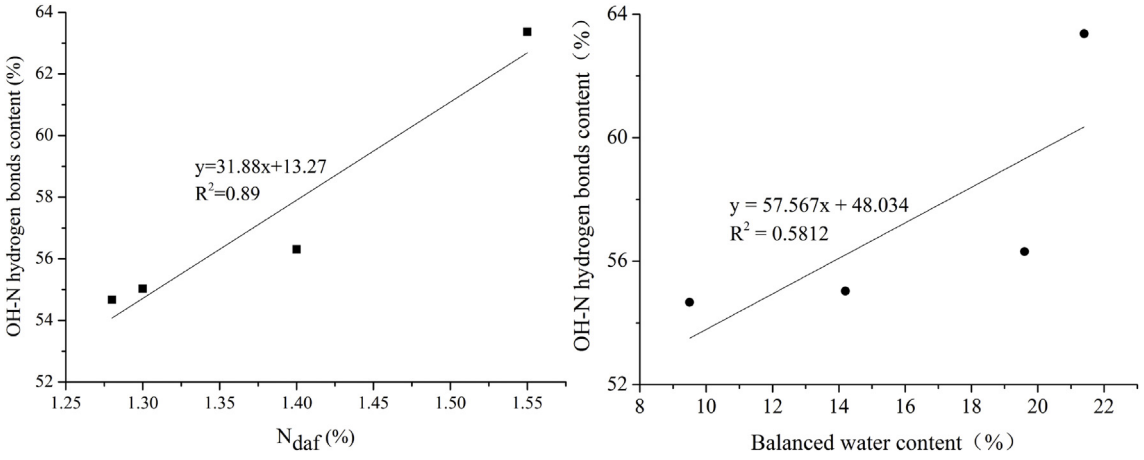

Fig. 7. The relationship between the content of OH-N hydrogen bond and N_{daf}, balanced water content.

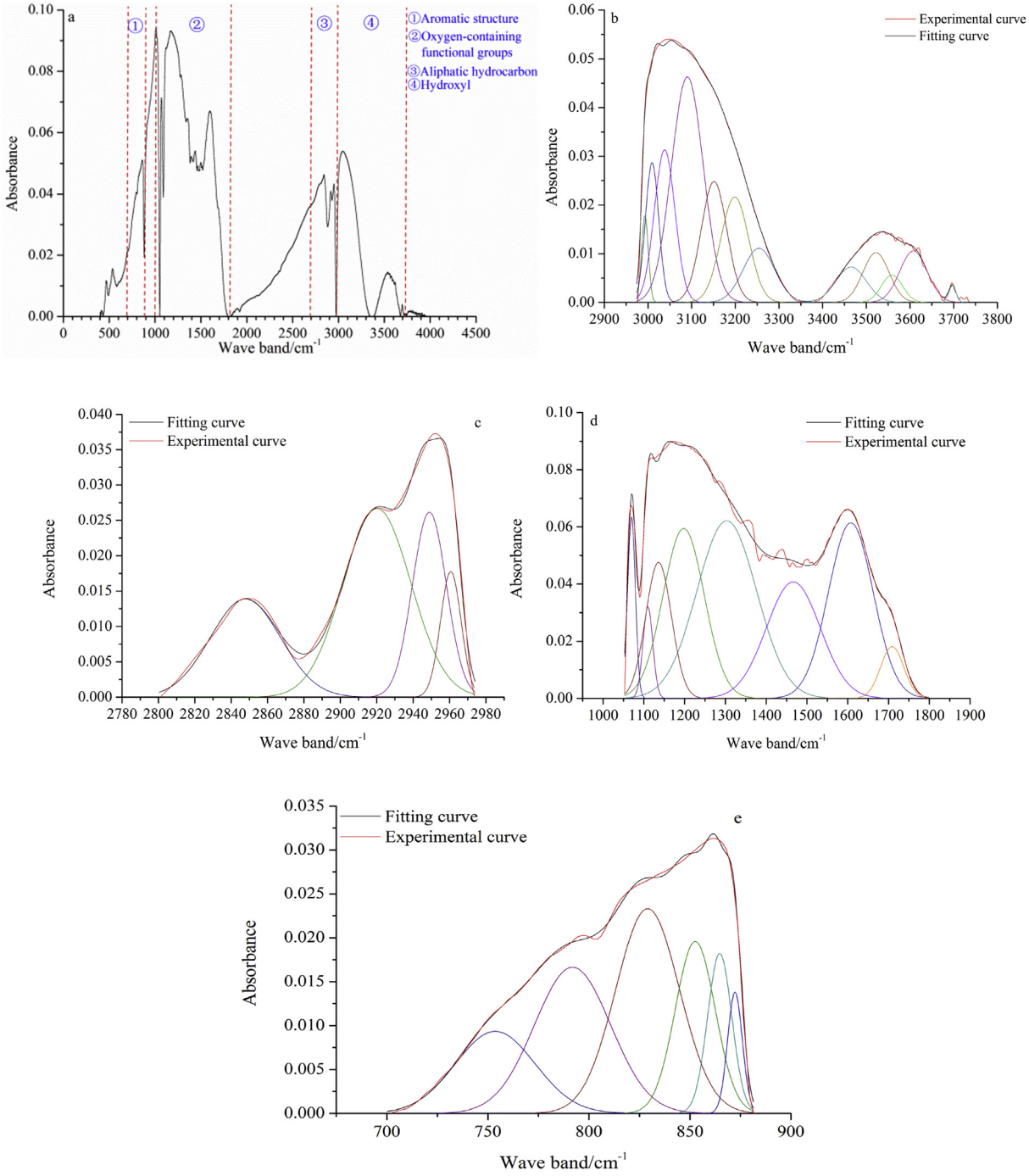

Fig. 8. Infrared spectrogram of raw coal.

Table 5
FTIR and ultimate analysis results.

Coal sample	Ultimate analysis/%				$R_{o,max}$/%	Balanced water content/%	OH-N hydrogen bond content/%
	O_{daf}	C_{daf}	H_{daf}	N_{daf}			
B-3b	25.27	70.99	1.1	1.55	0.35	21.4	63.37
S-5a	27.01	69.5	0.93	1.4	0.41	19.6	56.31
S-5b	25.56	71.88	0.48	1.3	0.32	14.2	55.03
H-14	23	74.63	0.86	1.28	0.32	9.5	54.67

formation condition. Therefore, kaolinite can adhere to the surface of a coal matrix. After being replaced by low salinity salt water, the repulsion between kaolinite and the coal matrix increases due to the expansion of the double layer, so that kaolinite is released from the surface of the coal matrix (Han et al., 2008). Wang et al. (2001) proposed that the pH value of the solution has an effect on the charge of clay minerals. It is shown that the number of variable negative charges of clay minerals increases with the increase of pH under alkaline conditions. Under acidic conditions, positive charges can be generated on the end surface of clay minerals, and the number of positive charges increases with the decrease in pH. Under the alkaline condition, the increase of the negative charge on the clay surface leads to an increase of the repulsion force of the double layer, and the clay minerals such as kaolinite are more easily released from the surface of the coal matrix. By contrast, the weakening of the repulsion of the double electron layer

Table 6
Absorption peak parameters of hydroxyl absorption band by peak fitting.

Number	Peak position/cm^{-1}	half-peak width/cm^{-1}	Area	Relative area/%	Ascription
1	2993.01	18.08	0.34	2.32	OH-N hydrogen bonds
2	3009.39	35.68	1.08	7.36	OH-N hydrogen bonds
3	3038.16	55.37	1.84	12.53	OH-N hydrogen bonds
4	3090.14	85.84	4.23	28.78	OH-N hydrogen bonds
5	3151.17	68.84	1.82	12.38	hydrogen bonds of ring structure
6	3198.69	75.12	1.73	11.78	hydrogen bonds of ring structure
7	3253.92	85.49	1.01	6.89	OH-ether hydrogen bonds
8	3465.33	81.53	0.63	4.29	Self associating hydroxyl
9	3522.16	70.27	0.76	5.21	OH-π hydrogen bonds
10	3558.66	56.78	0.34	2.31	OH-π hydrogen bonds
11	3607.96	73.98	0.83	5.67	free OH hydrogen bond
12	3697.26	18.81	0.07	0.47	Water in silicate minerals

makes the clay particles difficult to separate under acidic conditions. Therefore, kaolinite is easy to separate under partial alkaline conditions and the displacement pressure is large, making the water sensitivity of particle migration the strongest. Under the partial acidic condition, the stability between the coal matrix and particle is good and the displacement pressure is minimal, leading to no change of the permeability of the coal reservoir at this stage Although kaolinite is the easiest to release under the strong alkalinity condition, the displacement pressure is small; therefore, the particle migration of water sensitive is moderate.

As the salinity is further reduced, the damage rate of dimensionless permeability under varying pH values increases compared to the second stage, indicating that the volume of expansive clay minerals (such as illite/smectite mixed layer mineral) will expand dozens of times after contacting water. The porosity is blocked, the permeability is significantly reduced, and the water sensitivity of particle expansion is more serious than that of particle migration (Fig. 9c). The surfaces of the clay mineral particles carry residual negative charges as a result of isomorphous substitution and the broken bonds that occur at the edges of particles. Layers of water molecules are held around the clay mineral particle by hydrogen bonding and by the dipole character of the water molecules. In addition to the adsorption of water molecules, cations are also attracted to the clay mineral particle. The net effect is that cations form a dispersed layer adjacent to the clay particle but the cation concentration decreases with increasing distance from the clay surface, as illustrated in Fig. 13 (Zhang et al., 2015). Due to the charge on the surface of clay minerals it is easy to form electric double layers in aqueous solution, including stern and diffusion layers, and the outer layer is the free layer (Fig. 12). There are four water adsorption centres (complex triangle cell of the base surface, oxygen atom and hydroxide ions of the base surface, interlayer exchangeable cations, unbalanced ion cast on the side of the fracture) on the surface of clay minerals with varying adsorption energy. The water in the stern layer is adsorbed water, and the water in the diffusion layer is seepage water. The adsorbed water has high viscosity and shear force, which is quite different from those of free water. The clay minerals of the experimental samples are dominated by kaolinite and illite/smectite mixed layer mineral. The former represents swelling clay minerals and the latter represents non-swelling clay minerals. Both have similar structures composed of a 2D array of an aluminium/oxygen/hydroxyl octahedral sandwiched between 2D arrays of silica/oxygen tetrahedrals (tetrahedral-octahedral-tetrahedral). For the illite/smectite mixed layer mineral, trivalent Al is substituted by tetravalent Si and divalent cations are substituted on the interlayer surface. The distance between the two structured layers, d_{100} spacing, is a function of the characteristics of the exchangeable cations, composition of the solution, and clay mineralogy. In the presence of water, interlayer exchangeable cations have the tendency to hydrate and to increase the d_{100} spacing, which results in a volume expansion that is referred to as clay swelling. For kaolinite, lattice substitutions mostly occur in the tetrahedral layer. The compensating interlayer cations unlike the cations on the external surface, are not generally exchangeable. Thus, interlayer swelling by water is not observed in kaolinite compared with illite/smectite mixed layer minerals (Sanaei et al., 2017).

M_2 is the demarcation point of the second stage and third stage, indicating that when the salinity is higher than 1250 mg/L, due to the ions from the unbalanced electricity on the side of the fracture, high specific adsorption cations in the fluid lead to a reversal of the electricity on the clay minerals. The Zeta potential of clay minerals is positive under the conditions of a high salinity and pH in the scope of the experiment (pH is between 6 and 10); the double layer is compressed and the hydration expansion is not obvious. Alternatively, when the electrolyte concentration sharply decreases, the hydration expansion is significant (Yu et al., 2011). The effect of pH on the hydration and expansion of clay minerals is influenced by the charge of clay particles. The amount of adsorbed ions on clay particles depends on the number of charges. Permanent negative charges of clay minerals are distributed on the crystal plane of layered aluminosilicates and are balanced by exchangeable cations, such as K^+, Na^+, Ca^{2+}, Mg^{2+}, and H^+. This balance is maintained by positive and negative electrostatic attraction. The number of variable negative charges in clay minerals varies with the pH value of the medium. The hydroxyl groups in the clay mineral crystals dissociate H^+ in an alkaline medium, causing the clay particles to be negatively charged. Moreover, in an alkaline medium, the dissociation of Al^{3+} exposed on the surface of the clay particles causes the surface to be negatively charged (Tchistiakov, 2000; Wang et al., 2001). The amount of variable negative charge increases as the pH increases. When the medium is acidic, a positive charge can be generated on the end face of the clay particle and the amount of positive charge increases as the pH value decreases. The change in the charge of clay minerals due to the change in the pH of the medium ultimately affects the hydration and expansion of clay minerals because the charge on the

Table 7
Absorption peak parameters of aliphatic carbocycle by peak fitting.

Number	Peak position/cm^{-1}	half-peak width/cm^{-1}	Area	Relative area/%	Ascription
1	2847.84	45.67	0.67	24.13	Symmetrical telescopic vibration of CH_2
2	2948.95	22.06	0.61	22.06	Asymmetric telescopic vibration of CH_3
3	2960.69	13.37	0.25	9.03	Asymmetric telescopic vibration of CH_3
4	2920.16	43.83	1.24	44.78	Asymmetric telescopic vibration of CH_2

Table 8
Absorption peak parameters of oxygen-containing functional groups by peak fitting.

Number	Peak position/cm^{-1}	half-peak width/cm^{-1}	Area	Relative area/%	Ascription
1	1069.78	22.20	1.44	3.47	Alkyl ether
2	1109.93	28.60	0.97	2.35	C-O vibration of ether
3	1136.08	74.42	3.75	9.03	C-O vibration of hydroxyl benzene and ether
4	1197.74	119.19	7.53	18.11	C-O vibration of hydroxyl benzene and ether
5	1303.31	172.09	11.38	27.39	C-O vibration of aryl ether
6	1607.56	129.17	8.44	20.32	C=C framework vibration of aromatic hydrocarbons
7	1709.00	66.69	1.29	3.09	C=O expansion vibration of unsaturated carboxylic acid
8	1466.55	155.68	6.75	16.24	Deformable vibration of -$CH_3$and -CH_2

surface of clay minerals makes it easy to form an electric double layer in aqueous solution, including a stern and diffusion layer; the outer layer is the free layer (Fig. 12). The Zeta potential is commonly used to reflect the thickness of the electric double layer and water film (Gregory and O'Melia, 1989; Olphen et al., 1978). As a positive charge can be generated on the end face of the clay particle under acidic conditions, the Zeta potential of clay minerals is positively charged. The electric double layer is compressed, and the water film thickness is reduced (Fig. 13). On the contrary, under alkaline conditions, the Zeta potential significantly decreases and the water film thickness is increased (Fig. 13). It is observed that a low pH value of the fluid inhibits the swelling of the clay, while a high pH value enhances the swelling of the clay.

In this experiment, the change rate of dimensionless permeability decreases with the increase of pH, indicating that the permeability damage rate is affected by the water sensitivity of the particle expansion and other factors. Since the inorganic minerals in coal occupy a small part, the composition of pulverized coal is not only composed of minerals, and further consideration must be given to the combination of organic microscopic components. The movement of particles is affected by wettability according to the theory of particle migration. The DLVO theory shows that the factors that affect the wettability of the coal surface are mainly the Zeta potentials at the solid/water interface. The smaller the Zeta potential, the more negative charges on the solid surface and the more stable the water film, which has stronger hydrophilicity of the salt water (Oyeneyin et al., 1995; Yang et al., 2015). In an alkaline environment, more active hydrogen ions will be dissociated on the surface of the coal, and the negative charge on the coal surface will increase. The electromotive force is defined as the zeta potential produced by the formation of electric double layers on the coal surface and the surrounding medium (Li et al., 2014). The negative value of the electromotive force increases with the increase of pH, and the hydrophilicity of the coal increases (Fig. 10) (Li et al., 2014). In a weak acid environment, the number of hydrogen ions around the coal sample increases, and the negative charge amount of coal surface is reduced. The absolute value of electromotive force decreases, and the hydrophilicity of coal rock is weakened (Li et al., 2014). Therefore, pulverized coal particles encounter difficulty when migrating from acidic conditions to strong alkali condition in the fluid environment., and the displacement pressure under acidic conditions is the minimum. Therefore, pulverized coal particles are easy to agglomerate under the comprehensive influence, leading to the fastest decline of the non-dimensional permeability. In the third stage, the damage rate of permeability mainly depends on the joint action of the wettability of pulverized coal particles and expansion of clay hydration, The wettability of pulverized coal particles has the higher influence of the two.

3.4. Salt sensitive damage and its mechanism

The results of the salt sensitivity experiment show that the dimensionless permeability increases with the increase of the salinity under the partial acidity condition. Under alkaline conditions, the reservoir does not exhibit weak salt sensitivity, and the greater the alkalinity, the stronger the salt sensitivity (Fig. 11). The charge on the surface of clay minerals make it easy to form electric double layers in aqueous solution, including the stern and diffusion layers, and the outer layer is the free layer (Fig. 12). The water in the stern layer is adsorbed water, and the water in the diffusion layer is seepage water. The adsorbed water has a high viscosity and shear force, which is quite different from those of free water. When the clay particles move relative to the solution, they form a shear plane. The potential on the shear plane is called the Zeta potential, which can reflect the thickness of the electric double layer and water film. Under the experimental conditions (pH is between 6 and 10), the Zeta (ζ) potential increases with the increase of salinity(Fig. 12) (Yu et al., 2011). With the increase of the salinity of the fluid, some of the cations in the diffusion layer enter the stern layer to help balance the negative charge on the mineral surface. When the salinity is high enough, the negative charge on the base surface of the clay minerals is basically balanced, and the Zeta potential is very low. Due to the existence of variable charges on the side, the high specific adsorbed cation in the fluid causes electrical inversion, and the surface of the clay minerals is positively charged. Therefore, the Zeta potential of clay minerals is positively charged, the electric double layer is compressed, and the water film thickness is reduced(Gregory and O'Melia, 1989; Olphen et al., 1978). Under the condition of partial acidity (pH = 6), H^+ can also participate in the electric balance of clay mineral base surface as an exchangeable cation. As the value of the Zeta (ζ) potential reaches the maximum (Fig. 13) so that the electric double layer is compressed, the thickness of water film and the resistance of fluid flow decreases, increasing the permeability of liquid. Under alkaline conditions, the zeta potential is negatively correlated with pH due to the presence of hydroxyl ions (Fig. 13). The increased thickness of the water film leads to a decrease of permeability. Especially under strong alkali conditions, the Zeta potential decreases significantly, and the increase of the water film thickness leads to a significant decrease in

Table 9
Absorption peak parameters of aromatic structure by peak fitting.

Number	Peak position/cm^{-1}	half-peak width/cm^{-1}	Area	Relative area/%	Ascription
1	753.65	46.36	0.46	15.07	Two substitution of benzene ring (4H)
2	791.89	44.34	0.79	27.77	Three substitution of benzene ring (3H)
3	829.06	37.14	0.92	30.21	Four substitution of benzene ring (2H)
4	852.61	23.27	0.48	15.89	Five substitution of benzene ring (1H)
5	864.72	14.12	0.27	8.95	Five substitution of benzene ring (1H)
6	872.28	8.63	0.13	4.13	Five substitution of benzene ring (1H)

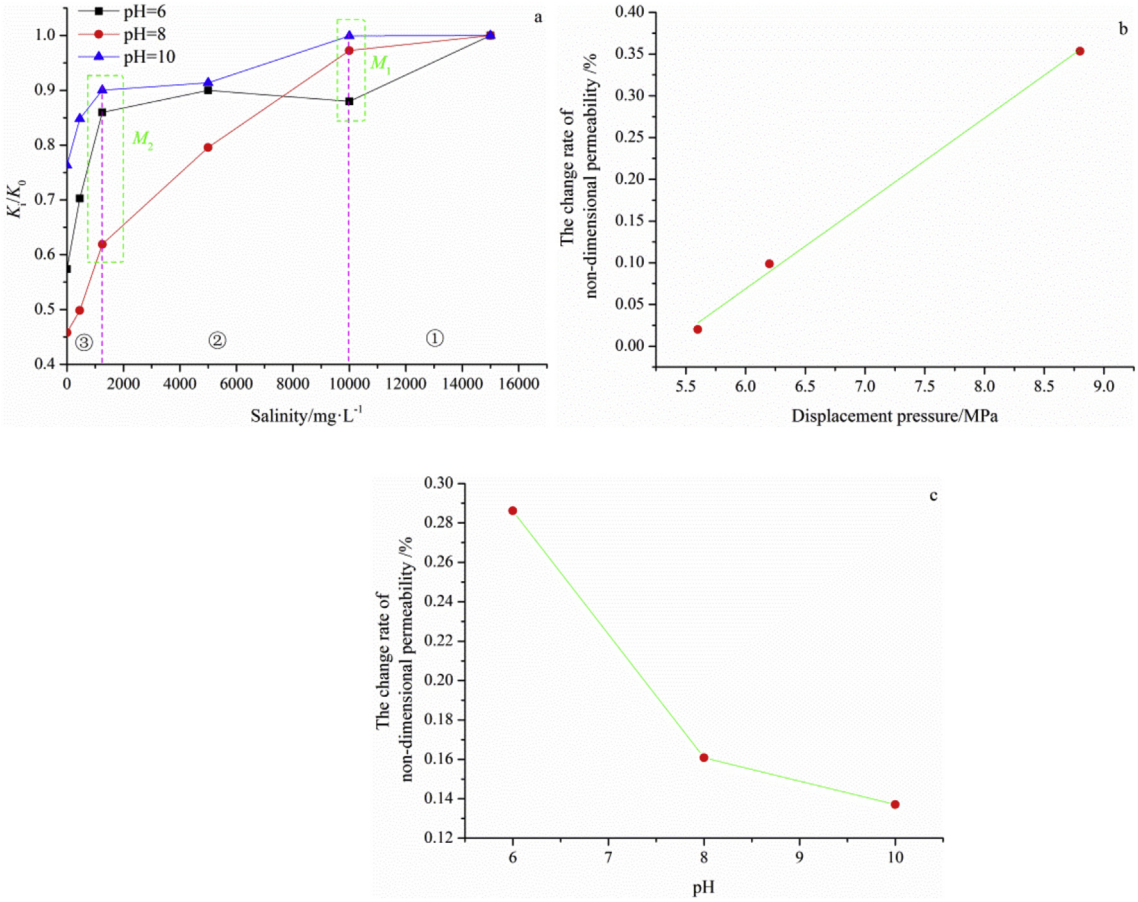

Fig. 9. Water sensitive effect under different pH.

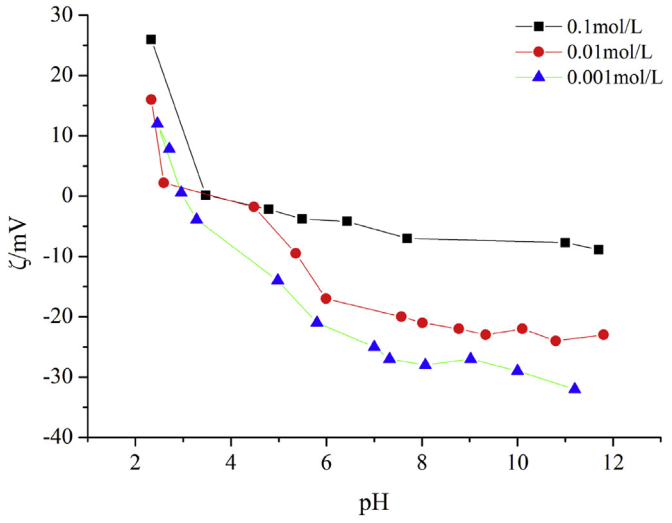

Fig. 10. The relationship between zeta potential of coal surface and pH under different salinity.

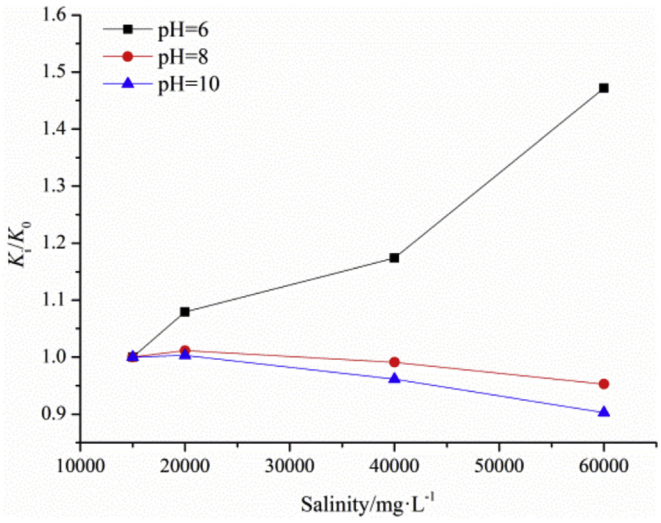

Fig. 11. Salt sensitive effect under different pH.

permeability (Yu et al., 2011).

3.5. Recommendations

The damage caused by the external fluid to the coal reservoir occurs in the process of the whole coal seam gas drainage, of which the agglomeration of pulverized coal and the hydration and expansion of clay minerals are important factors for blocking the passage of fluid (Lehman et al., 1998; Zou et al., 2014). The former is mainly influenced by temperature, particle size distribution and coal metamorphism, and the latter is influenced by the mineral content, occurrence of clay minerals and pore characteristics of the reservoir, but both are controlled by external factors (pH and the velocity of flow). Based on the DLVO theory, the water sensitivity (salt sensitivity) mechanism of the lignite reservoir under the interaction of pH and the velocity of flow is discussed in this paper (Shi et al., 2018).

From the above experiments, it can be concluded that water

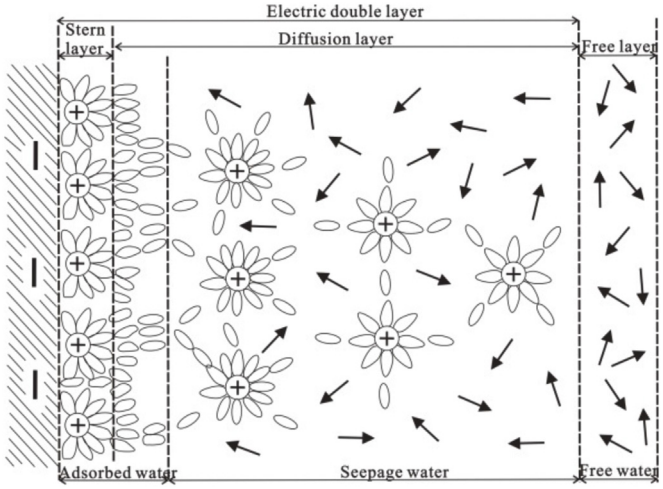

Fig. 12. Water film structure on the surface of clay mineral.

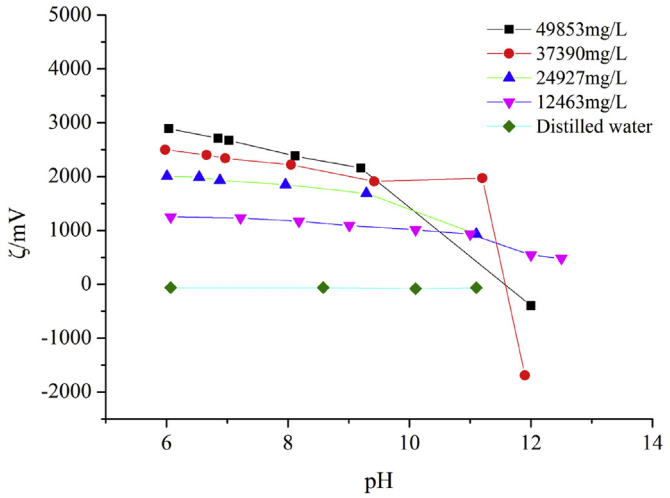

Fig. 13. The relationship between zeta potential of clay mineral and pH under different salinity.

sensitive damage aggravates the microscopic and macroscopic heterogeneity of the pore structure and then affects the permeability of the reservoir. No matter what type of pH injection solution is used, KCl and other stabilizers should be added to prevent the swelling and hydration of clay minerals. Additionally, the rate of liquid injection should be reduced to suppress the water sensitivity of particle migration. Under the same displacement pressure difference, an increase of alkalinity is beneficial to reduce the production of water sensitive damage, but it should not be too high. Because of the strong alkali - sensitive mineral quartz in coal, alkali - sensitive damage of the coal reservoir will be caused by high alkalinity. At the same time, a high-alkaline injection solution will dissolve the proppant such as quartz sand to reduce the support effect, which will result in a significantly lower permeability. Therefore, in the fracturing stage of coalbed methane wells, the properties of the fracturing fluid can be reasonably changed to improve the wettability of pulverized coal, thereby increasing the gas production rate.

The salt sensitivity characteristics at different pH values indicate that injecting a highly acidic solution with a more acidic solution will help reduce the fluid flow resistance. The primary reason for this reduction is that although pulverized coal tends to agglomerate under partial acidity conditions, it is more conducive to the fixation of coal sources under high salinity conditions. Therefore, it is more favorable for the seepage of the coal reservoir under the appropriate injection rate of the external liquid.

4. Conclusion

The minerals in coal are dominated by clay minerals, followed by quartz, and other mineral content is less. The clay minerals are dominated by kaolinite and illite/smectite mixed layer. Different occurrence types of clay minerals have different effects on water sensitivity. The aromatic structure of lignite is mainly substituted by four substitution of benzene ring (2H) and five substitution of benzene ring (1H). Aliphatic hydrocarbons are mainly in the form of long chain. The ratio of the carbonyl, hydroxyl benzene and carboxyl is 10:7:1. The hydrogen bond is dominated by OH-N hydrogen bond.

The lignite reservoirs with different pH have different degrees of water-sensitive damage. Partial alkalinity conditions and partial acidity conditions are strong water sensitive, and strong alkalinity conditions is weak water sensitive. The dimensionless permeability changes with the decrease of salinity, which can be divided into three stages with 1250 mg/L and 10000 mg/L as the boundary. In no water sensitivity stage, the change of dimensionless permeability depends on the wettability changes of pulverized coal under the influence of pH. In particle migration water sensitivity stage, the permeability damage rate is mainly controlled by the change of displacement pressure and double layer repulsion force. In the particle expansion water sensitivity stage, the Permeability damage rate mainly depends on the effect of the wettability of pulverized coal particles and the hydration and expansion of clay minerals, of which the former is higher than the latter.

The dimensionless permeability of lignite reservoir increases with the increase of salinity under the partial acidity condition. Under alkaline conditions, it is characterized by no-weak salt sensitivity. The greater the alkalinity, the stronger the salt sensitivity, which is mainly controlled by the change of the thickness of the water film under the influence of pH.

Acknowledgments

The project was financially supported by the Key Laboratory of Coalbed Methane Resources and Reservoir Formation Process of the Ministry of Education (China University of Mining and Technology) (No.2018-005), the Fundamental Research Funds for the Central Universities (2015XKZD07), and National Science and Technology Major Project (2016ZX05041-001).

References

Bai, J.P., 2014. Influence of high-rank coal reservoir sensitivity on coalbed methane wells production. Coal Sci. Technol. 42 (12), 54–57.
Cuntian, C.Q., 1992. Study on Wettability of Coal and its Application. China Coal Industry Publishing House, Beijing.
Chen, Y., Mastalerz, M., Schimmelmann, A., 2012. Characterization of chemical functional groups in macerals across different coal ranks via micro-FTIR spectroscopy. Int. J. Coal Geol. 104 (1), 22–33.
Chen, W.M., 1988. Distribution of nitrogen in Chinese coal and its calculation formulae. Coal Sci. Technol. 16 (4), 20–26.
Deng, C.M., 2015. Coalbed methane reserve mechanism and insitu gas content modeling in low rank coal reservoir. China Univ. Geosci. (Beijing) 1–134.
Geng, Y.G., Tang, D.Z., Xu, H., Tao, S., Tang, S.L., Ma, L., Zhu, X.G., 2017a. Experimental study on permeability stress sensitivity of reconstituted granular coal with different lithotypes. Fuel 202, 12–22.
Geng, Y.G., Tang, D.Z., Xu, H., Tao, S., Tang, S.L., 2017b. Pore cracking features of coal reservoir in Anze Block and water sensitive effect failure mechanism. Coal Sci. Technol. 45 (5), 175–180.
Gregory, J., O'Melia, C.R., 1989. Fundamentals of flocculation. Crit. Rev. Environ. Sci. Technol. 19 (3), 185–230.
Han, D.J., Dong, P.C., Shi, N., 2008. Sensitivity experiment study and its mechanism analysis of the oil reservoirs. Pet. Geol. Oilfield Dev. Daqing 27 (5), 14–17.
Huang, G.L., Cheng, H., Luo, D.G., Zhou, W.B., 2005. Hydrogeochemical characteristics of groundwater in Hami depression. Uranium Geol. 21 (2), 97–104.
Huang, S.P., Liu, D.M., Yao, Y.B., Gan, Q., Cai, Y.D., Xu, L.L., 2017. Natural fractures initiation and fracture type prediction in coal reservoir under different in-situ stresses during hydraulic fracturing. J. Nat. Gas Sci. Eng. 43, 69–80 2017.
He, X., Liu, X., Nie, B., Song, D.Z., 2017. FTIR and Raman spectroscopy characterization

of functional groups in various rank coals. Fuel 206, 555–563.
Jozanikohan, G., Sahabi, F., Norouzi, G.H., Memarian, H., Moshiri, B., 2016. Quantitative analysis of the clay minerals in the Shurijeh Reservoir Formation using combined X-ray analytical techniques. Russ. Geol. Geophys. 57 (7), 1048–1063.
Khilar, K.C., Fogler, H.S., 1984. The existence of a critical salt concentration for particle release. J. Colloid Interface Sci. 101 (1), 214–224.
Li, X.C., Kang, Y.L., Yin, Z.S., 2014. Surface electricity and wettability of coal rock under the condition of different chemical environments. J. China Univ. Min. Technol. 43 (5), 864–869.
Li, J.Q., Liu, D.M., Yao, Y.B., Cai, Y.D., Chen, Y., 2013. Evaluation and modeling of gas permeability changes in anthracite coals. Fuel 111, 606–612.
Liao, J., Tang, H.M., Zhu, X.M., Ren, M.Y., Sun, Z., Lin, D., 2012. Water sensitivity experiment and damage mechanism of sandstone reservoirs with ultra-low permeability:a case study of the eighth oil layer in the Yanchang Formation of Xifeng oilfield. Ordos Basin 33 (2), 321–328.
Lehman, L.V., Blauch, M.E., Robert, L.M., 1998. Desorption enhancement in fracture-stimulated coalbed methane wells. J. Petrol. Technol. 51 (4), 101–102.
Liu, X.Y., Liu, Y.S., Xia, Y.C., 2017. Calorimetry investigation on wettability and moisture Re-adsorption of lignite. Coal Convers 40 (3), 8–14.
Ma, K., Jiang, H.Q., Li, J.J., Zhao, L., 2016. Experimental study on the micro alkali sensitivity damage mechanism in low-permeability reservoirs using QEMSCAN. J. Nat. Gas Sci. Eng. 36, 1004–1017.
Moghanloo, R.G., Dadmohammadi, Y., Bin, Y., Salahshoor, S., 2015. Applying fractional flow theory to evaluate CO $_2$, storage capacity of an aquifer. J. Petrol. Sci. Eng. 125, 154–161.
Machnikowska, H., Krztoń, A., Machnikowski, J., 2002. The characterization of coal macerals by diffuse reflectance infrared spectroscopy. Fuel 81 (2), 245–252.
Oyeneyin, M.B., Peden, J.M., Hosseini, A., Ren, G., 1995. Factors to consider in the effective management and control of fines migration in high permeability sands. In: Paper SPE 30112 Presented at the SPE European Formation Damage Conference, the Hague, pp. 345–349.
Olphen, V., Hsu, H., Ho, P., 1978. An introduction to clay colloid chemistry. Soil Sci. 97 (4), 290.
Painter, P.C., Sobkowiak, M., Youtcheff, J., 1987. FT - IR study of hydrogen bonding in coal. Fuel 66 (7), 973–978.
Pietrzak, R., Wachowska, H., 2006. The influence of oxidation with HNO 3 on the surface composition of high-sulphur coals: XPS study. Fuel Process. Technol. 87 (11), 1021–1029.
Robertson, J., 2004. Raman spectroscopy of amorphous, nanostructured, diamond-like carbon, and nanodiamond. Philos. T. 362 (1824), 2477.
Shi, Q.M., Qin, Y., Zhou, B.Y., Zhang, M.J., Wu, M., Wang, L.N., 2018. An experimental study of the agglomeration of coal fines in suspensions: inspiration for controlling fines in coal reservoirs. Fuel 211, 110–120.
Sanaei, A., Shakiba, M., Varavei, A., Sepehrnoori, K., 2017. Mechanistic modeling of clay swelling in hydraulic-fractures network. In: SPE Western Regional Meeting, pp. 1–13.
Tan, C., Richards, B., Rahman, S., Andika, R., 1997. Effects of swelling and hydrational stress in shales on wellbore stability. In: SPE Asia Pacific Oil and Gas Conference and Exhibition. Society of Petroleum Engineers, U of New South Wales, Sydney, Australia, pp. 345–349.
Tchistiakov, A.A., 2000. Colloid chemistry of in-situ clay-induced formation damage. In: SPE International Symposium on Formation Damage Control Held in Lafayette, Louisiana, pp. 1–9.
Tao, S., Tang, D.Z., Xu, H., Yi, C., Geng, Y.G., Zhao, J.L., Wu, S., Meng, Q., Kou, X., Yang, S.Y., Yi, C., 2017. Fluid velocity sensitivity of coal reservoir and its effect on coalbed methane well productivity: a case of Baode Block, northeastern Ordos Basin, China. J. Petrol. Sci. Eng. 229–237.
Wang, W.Y., Tang, Z.H., Lv, Y.H., Du, Y., Zhao, L., 2001. Influencing factors of water sensitivity in reservoir rock. J. Jianghan Petrol. Ins. 23 (2), 49–50.
Wang, K.X., 2010. Physical Simulation and Numerical Simulation of Adsorbed State, Solubel State and Free State Gas Volume in Low Rank Coal Reservoir. China Uni. Min. Techno.
Wang, B.Y., Qin, Y., Shen, J., Wang, G., Zhang, Q.S., 2018. Influence of stress and formation water properties on velocity sensitivity of lignite reservoir using simulation experiment. Fuel 224, 579–590.
Wei, X., 2014. Rearch in Reservoir Characteristic and Reservoir Sensitivity of the Member 8 in Zhao 30 Wellblock, Ordos Basin. Chengdu Univ. Tech.
Wu, S., Tang, D.Z., Li, S., Wu, H.Y., Hu, X., Zhu, X.G., 2017. Effects of geological pressure and temperature on permeability behaviors of middle-low volatile bituminous coals in eastern Ordos Basin, China. J. Petrol. Sci. Eng. 153, 372–384.
Yang, Y., Cao, Y., Tian, H.J., Li, D., Zhang, H., Sun, H.S., Wu, X., Chen, W.G., 2015. Mechanism anlaysis of coal fines damaged to coal reservoirs and prevention countermeasures during fracturing. Coal Sci. Technol. 43 (2), 84–87.
Yu, Y.F., Kang, Y.L., You, L.J., 2011. Thickness change of water film-new mechanism of salt sensitivity in extra-low permeability sandstone reservoirs. J. Chongqing Univ. (Nat Sci Ed) 34 (4), 67–71.
Zhang, J., Zhu, D., Hill, A.D., 2015. Water-induced fracture conductivity damage in shale formations. In: SPE Hydraulic Fracturing Technology Conference, pp. 1–17.
Zhang, Y., Wang, J., Xue, S., Wu, J.M., Chang, L.P., Li, Z.F., 2016. Kinetic study on changes in methyl and methylene groups during low-temperature oxidation of coal via in-situ FTIR. Int. J. Coal Geol. 154–155, 155–164.
Zuo, Y.Q., Zhang, X.Y., Zhou, R., Li, S., 2014. Water sensitivity and its controlling factors on high-rank coal reservoirs in southern Qinshui basin. Petro. Geo. Recov. Effic. 21 (5), 107–110.
Zhu, Y.S., Qu, H.Z., Lin, F.X., Wu, C.P., Han, Y.Y., 2004. Seepage flow characters of oil displacement with water drive in water-sensitive formation of Mubo Yan10 reservoir. Acta Petrol. Sin. 25 (2), 59–64.
Zhu, Y.M., Zhao, X.F., Gao, L.J., Cheng, J.X., 2018. Quantitative analysis of structural changes on refined coal tar pitch with curve-fitted of ftir spectrum in thermal conversion process. Spectrosc. Spectr. Anal. 38 (7), 2076–2080.
Zou, Y.S., Zhang, S.C., Zhang, J., 2014. Experimental method to simulate coal fines migration and coal fines aggregation prevention in the hydraulic fracture. Transport Porous Media 101 (1), 17–34.